INFECTION AND IMMUNITY, Dec. 2009, p. 5233–5244 Vol. 77, No. 12
0019-9567/09/$12.00 doi:10.1128/IAI.00665-09


# Bcl-2 Regulates the Onset of Shiga Toxin 1-Induced Apoptosis in THP-1 Cells[▽]

Moo-Seung Lee, Rama P. Cherla, Dinorah Leyva-Illades, and Vernon L. Tesh*

*Department of Microbial and Molecular Pathogenesis, Texas A&M University System Health Science Center, College Station, Texas 77843-1114*

Received 10 June 2009/Returned for modification 7 July 2009/Accepted 3 September 2009

**Shiga toxins (Stxs), which are proteins expressed by the enteric pathogens *Shigella dysenteriae* serotype 1 and some serotypes of *Escherichia coli*, are potent protein synthesis inhibitors. Stx-producing organisms cause bloody diarrhea with the potential to progress to acute renal failure and central nervous system complications. Studies using animal models of these diseases have shown that Stxs are major virulence factors, and purified toxins have been shown to be capable of killing many types of cells in vitro. We showed that Stx type 1 (Stx1) rapidly induced apoptosis in undifferentiated, monocytic THP-1 cells through a mechanism involving the endoplasmic reticulum (ER) stress response. Rapid apoptosis correlated with increased expression of C/EBP homologous protein (CHOP), TRAIL, and DR5, while expression of the antiapoptotic factor Bcl-2 was downregulated. Stx1 treatment of differentiated, macrophage-like THP-1 cells was associated with cytokine production and delayed apoptosis. The mechanisms contributing to cell maturation-dependent differences in responses to Stx1 are unknown. We show here that in macrophage-like cells, Stx1 activated the proximal ER stress sensors RNA-dependent protein kinase-like ER kinase and inositol-requiring ER signal kinase 1α but did not activate activating transcription factor 6. Proapoptotic signaling pathways mediated by CHOP and by Bax and Bak were activated by Stx1. However, the toxin also activated prosurvival signaling through increased expression, mitochondrial translocation, and alternative phosphorylation of Bcl-2.**

Shiga toxins (Stxs), also called Shiga-like toxins or verotoxins, are potent protein synthesis inhibitors expressed by the enteric pathogens *Shigella dysenteriae* (serotype 1) and *Escherichia coli* (select serotypes). Stxs act as virulence factors by increasing the severity of bloody diarrhea and increasing the likelihood of development of life-threatening postdiarrheal sequelae, such as acute renal failure (hemolytic-uremic syndrome) and central nervous system complications (40). *S. dysenteriae* serotype 1 expresses the prototypic Stx, while closely related toxins expressed by *E. coli* can be classified into Stx type 1 (Stx1) and Stx2 (30). X-ray crystallographic analyses revealed that all Stxs contain six protein subunits in an arrangement described as an $AB_5$ structure. Stx A-subunits possess *N*-glycosidase activity that depurinates a specific unpaired adenine residue from eukaryotic rRNA, leading to protein synthesis inhibition in the intoxicated cell (11, 35). The pentameric B-subunits are responsible for toxin binding to the cell surface and interact with the neutral globo series glycolipid globotriaosylceramide (for a review, see reference 26). Toxin-mediated receptor cross-linking through interaction with the pentameric B-subunits is thought to trigger receptor-mediated endocytosis. Once internalized, the toxins are sequentially delivered from an early endosome to the trans-Golgi network, through the Golgi apparatus, to the endoplasmic reticulum (ER), and into the cytosol (for a review, see reference 34). The mechanisms of toxin retrograde transport and retrotranslocation across the ER membrane remain to be fully characterized. Nevertheless, numerous reports indicate that the ER is the ultimate cellular compartment for facilitated cytosolic delivery of Stxs.

In addition to its role in cotranslational transport of nascent polypeptides, the ER is the principal site for the correct folding of proteins destined to enter the secretory pathway. A "protein quality control" process which detects improperly folded proteins and attempts to mediate correct folding has been characterized. During the lifetime of a cell, the rates of protein translocation into the ER lumen may vary. Cells may encounter conditions such as DNA damage, glucose deprivation, disrupted calcium homeostasis, or hypoxia in which the capacity of the ER to correctly fold proteins becomes saturated, a condition referred to as ER stress (1, 10). Prolonged failure to correctly fold and translocate proteins from the ER can lead to induction of apoptosis (3, 32). Cells undergoing apoptosis display morphological changes such as cell membrane blebbing, cell shrinkage, and nuclear fragmentation that produce apoptotic bodies. ER stress-induced apoptosis is a critical factor in the pathophysiology of a number of clinical conditions, including Alzheimer's disease, Creutzfeldt-Jakob disease, Huntington's disease, cardiovascular dysfunction, and inflammatory bowel disease (20, 21).

Stxs initiate apoptotic cell death in vitro via induction of caspase-activated apoptotic signaling in many types of cells, including human epithelial, endothelial, and myeloid cells (for a review, see reference 4). Furthermore, renal epithelial cell apoptosis appears to be a characteristic of kidney damage in humans with hemolytic-uremic syndrome (19). We have previously shown that Stx1 induces apoptosis in the human myelogenous leukemia cell line THP-1 in a cell maturation-dependent manner (14).

* Corresponding author. Mailing address: Department of Microbial and Molecular Pathogenesis, 407 Reynolds Medical Building, Texas A&M University Health Science Center, College Station, TX 77843-1114. Phone: (979) 845-1313. Fax: (979) 845-3479. E-mail: tesh@medicine.tamhsc.edu.

▽ Published ahead of print on 14 September 2009.

Apoptosis is rapidly induced in undifferentiated, monocytic cells, whereas in differentiated, macrophage-like cells there is slow onset of apoptosis preceded by a period of increased protein synthesis and production of proinflammatory cytokines and chemokines. Rapid Stx1-induced apoptosis in monocytic cells was associated with activation of the ER stress response through the sensors RNA-dependent protein kinase-like ER kinase (PERK), inositol-requiring ER signal kinase 1α (IRE1α), and activating transcription factor 6 (ATF6). ER stress led to increased expression of the transcription factor C/EBP homologous protein (CHOP), the apoptosis-inducing factor TRAIL, and the death domain-containing receptor DR5, along with concomitant decreased expression of the prosurvival factor Bcl-2 (25). Some members of the Bcl-2 family, including Bcl-2 and Bcl-xL, act as antiapoptotic factors by inhibiting the mitochondrial uptake of $Ca^{2+}$ and blocking the release of cytochrome *c* from mitochondrial stores into the cytoplasm and the subsequent formation of the apoptosome. Other Bcl-2 proteins, such as Bax and Bak, are involved in apoptosis induction (7, 16). The mechanism(s) by which differentiation of THP-1 cells leads to transient increases in protein synthesis and delayed apoptosis following Stx treatment is unknown. We show here that, unlike treatment of monocytic cells with purified Stx1, which triggers primarily proapoptotic signaling cascades, treatment of macrophage-like THP-1 cells with purified Stx1 selectively activates the ER stress sensors PERK and IRE1α to relay both proapoptotic and prosurvival signals. The upregulated expression, mitochondrial translocation, and differential phosphorylation of the antiapoptotic factor Bcl-2 appear to be involved in the capacity of macrophage-like cells to initially survive intoxication with Stx1.

## MATERIALS AND METHODS

**Materials.** Antibodies directed against human phospho-PERK, phospho-eukaryotic initiation factor 2α (phospho-eIF-2α) ($Ser^{51}$), IRE1α, phospho-Bcl-2 ($Ser^{70}$, $Thr^{56}$), Bcl-2, Bcl-xL, Bax, Bak, BiP, and pan-actin were purchased from Cell Signaling Technology, Beverly, MA. Rabbit polyclonal anti-phospho-IRE1α ($Ser^{724}$) was purchased from Novus Biologicals, Inc., Littleton, CO. Anti-human ATF6 antibody was obtained from IMGENEX, San Diego, CA. Total PERK and CHOP (Gadd-153) antibodies were purchased from Santa Cruz Biotechnology Inc., Santa Cruz, CA.

**Cell culture.** The human myelogenous leukemia cell line THP-1 (American Type Culture Collection, Manassas, VA) was cultured in RPMI 1640 medium (Gibco-BRL, Grand Island, NY) containing 10% fetal bovine serum (HyClone Laboratories, Logan, UT), penicillin (100 U/ml), and streptomycin (100 μg/ml) at 37°C in 5% $CO_2$ in a humidified incubator. Cells maintained under these conditions were considered undifferentiated, monocytic cells. Monocytic cells ($1 \times 10^6$ cells/ml) were differentiated to the adherent macrophage-like state with phorbol 12-myristate 13-acetate (PMA) (Sigma Chemical Co., St. Louis, MO) at a concentration of 50 ng/ml for 48 h. Plastic-adherent cells were washed three times with cold, sterile Dulbecco's phosphate-buffered saline (Sigma Chemical Co., St. Louis, MO) and then incubated with fresh medium lacking PMA but containing 10% fetal bovine serum, penicillin (100 U/ml), and streptomycin (100 μg/ml). The medium was changed every 24 h for the next 3 days. Experiments were performed on the fourth day after PMA removal.

**Stxs.** Stx1 was expressed from *E. coli* DH5α(pCKS112), a recombinant strain harboring a plasmid containing the $stx_1$ operon under the control of a thermoinducible promoter (41). Cells were lysed, and periplasmic extracts were subjected to sequential ion-exchange and chromatofocusing chromatography. The purity of toxins was assessed by sodium dodecyl sulfate-polyacrylamide gel electrophoresis (SDS-PAGE) and Western blot analysis using anti-Stx1-specific antibodies. Prior to use, Stx1 preparations were shown to contain <0.1 ng of endotoxin/ml by use of the *Limulus* amoebocyte lysate assay (Associates of Cape Cod, East Falmouth, MA). Purified $Stx1A^-$, a holotoxin with two point mutations (E167Q and R170L) was a kind gift from Shinji Yamasaki, Osaka Prefecture University, Osaka, Japan. The site-directed mutations were shown to reduce toxin *N*-glycosidase activity by 5 logs (31). Purified pentameric Stx1 B-subunits were a kind gift from Cheleste Thorpe, Tufts University School of Medicine, Boston, MA.

**Total RNA extraction and semiquantitative RT-PCR.** Undifferentiated and differentiated THP-1 cells ($5 \times 10^6$ cells/well) were not treated or treated for 0 to 24 h with Stx1, $Stx1A^-$ (400 ng/ml), or thapsigargin (Tg) (10 μM) in RPMI 1640 medium with 10% fetal bovine serum. Following treatment, total RNA was isolated from cells using a phenol-free, filter-based RNA isolation system (RNAqueous kit; Ambion, Austin, TX) according to the manufacturer's instructions. Extracted total RNA was treated with RNase-free DNase at 37°C for 30 min to remove contaminating genomic DNA, and this was followed by heat inactivation at 95°C for 20 min. The RNA concentration and purity were determined by spectrophotometry (Nanodrop Technologies Inc., LLC, Wilmington, DE). Semiquantitative reverse transcription (RT)-PCR was performed using the AccessQuick RT-PCR system (Promega, Madison, WI) according to the manufacturer's protocol. The following target gene-specific PCR primers were used for the reactions: for human Bax, forward primer 5′-AAGCTGAGCGAGTGTCTCAAGCGC-3′ and reverse primer 5′-TCCCGCCACAAAGATGGTCACG-3′; for human Bak, forward primer 5′-TCCAGATGCCGGGAATGCACTGACG-3′ and reverse primer 5′-TGGTGGGAATGGGCTCTCACAAGG-3′; for human BiP, forward primer 5′-TAGCGTATGGTGCTGCTGTC-3′ and reverse primer 5′-TTTGTCAGGGGTCTTTCACC-3′; and for human β-actin, forward primer 5′-CTGTCTGGCGGCACCACCAT-3′ and reverse primer 5′-GCAACTAAGTCATAGTCCGC-3′. CHOP and Bcl-2 primers were designed as previously reported (25). Amplification of the expected single PCR product was confirmed using 1.5% agarose gels stained with ethidium bromide.

**Detection of XBP-1 mRNA splicing.** The method used for detection of unspliced and spliced X-box protein 1 (XBP-1) mRNA has been described previously (25). Briefly, RT-PCR products of XBP-1 mRNA were obtained from total extracted RNA using forward primer 5′-AAACAGAGTAGCAGCTCAGACTGC-3′ (sense) and reverse primer 5′-ATCTCTAAGACTAGGGGCTTGGT-3′ (antisense). Because a 26-bp fragment containing a PstI site is spliced upon activation of XBP-1 mRNA, the RT-PCR products were digested with PstI restriction enzyme to distinguish the active spliced form from the inactive unspliced form. Subsequent electrophoresis revealed that the inactive form is two cleaved fragments and the active form is a noncleaved fragment.

**Preparation of cellular lysates and Western blotting.** Eighteen hours prior to stimulation, differentiated THP-1 cells ($5 \times 10^6$ cells/well) were serum starved in RPMI 1640 medium containing 0.5% fetal bovine serum to reduce background kinase signaling. Cells were stimulated with Stx1 (400 ng/ml), $Stx1A^-$ (400 ng/ml), Stx1 B-subunit (800 ng/ml), or Tg (10 μm) for 0 to 24 h. Cells were harvested and lysed with modified radioimmunoprecipitation assay buffer (1.0% Nonidet P-40, 1.0% sodium deoxycholate, 150 mM NaCl, 50 mM Tris-HCl [pH 7.5], 0.25 mM sodium pyrophosphate, 2.0 mM sodium vanadate, 2.0 mM sodium fluoride, 10 μg/ml aprotinin, 1.0 μg/ml leupeptin, 1.0 μg/ml pepstatin, 200 mM phenylmethylsulfonyl fluoride) at 4°C. For detection of CHOP, cells were lysed with modified lysis buffer (137 mM NaCl, 15 mM EGTA, 0.1 mM sodium orthovanadate, 15 mM $MgCl_2$, 0.1% Triton X-100, 25 mM MOPS [morpholinepropanesulfonic acid] [pH 7.2], 100 mM phenylmethylsulfonyl fluoride, 20 μM leupeptin). Extracts were collected and cleared by centrifugation at 15,000 × *g* for 10 min. Cell lysates from monocytic THP-1 cells were prepared as previously described (25). The protein concentrations of each extract were determined using a Micro BCA protein assay kit (Pierce, Rockford, IL). Equal amounts of proteins (70 to 100 μg/lane) were separated by 8% or 12% Tris-glycine SDS-PAGE and transferred to nitrocellulose membranes. The membranes were blocked with 5% nonfat milk prepared with 20 mM Tris (pH 7.6)-137 mM NaCl-0.1% Tween 20. The membranes were incubated with primary antibodies at 4°C for 24 h. After washing, the membranes were incubated with horseradish peroxidase-labeled secondary antibodies for 2 h at room temperature. Bands were visualized using the Western Lightning chemiluminescence system (NEN-Perkins Elmer, Boston, MA). The data shown below are data from at least four independent experiments. Relative protein expression levels were measured using the NIH Image J software.

**Immunofluorescence confocal microscopy.** Differentiated and undifferentiated THP-1 cells were plated and cultured on eight-well LabTek chamber slides (Nalge Nunc International, Rochester, NY) at a density of $5 \times 10^4$ cells/well. Cells grown on chamber slides were treated with Stx1, $Stx1A^-$, or Stx1 B-subunits for 0 to 4 h. Cells were stained with MitoTracker Red (300 nM; Invitrogen, Eugene, OR) and then fixed with 4% paraformaldehyde for 15 min, permeabilized with 0.3% Triton X-100 for 4 min, and blocked with phosphate-buffered saline containing 1% bovine serum albumin. After two washes with phosphate-buffered saline for 2 min, polyclonal rabbit anti-human Bax-, Bak-, or Bcl-2-specific antibodies in blocking buffer were added to the slides, and the cells were incubated in humidified 5% $CO_2$ at 37°C for 2 h. After washing, fluorescein-conjugated goat anti-rabbit antibody (Vector Labo-

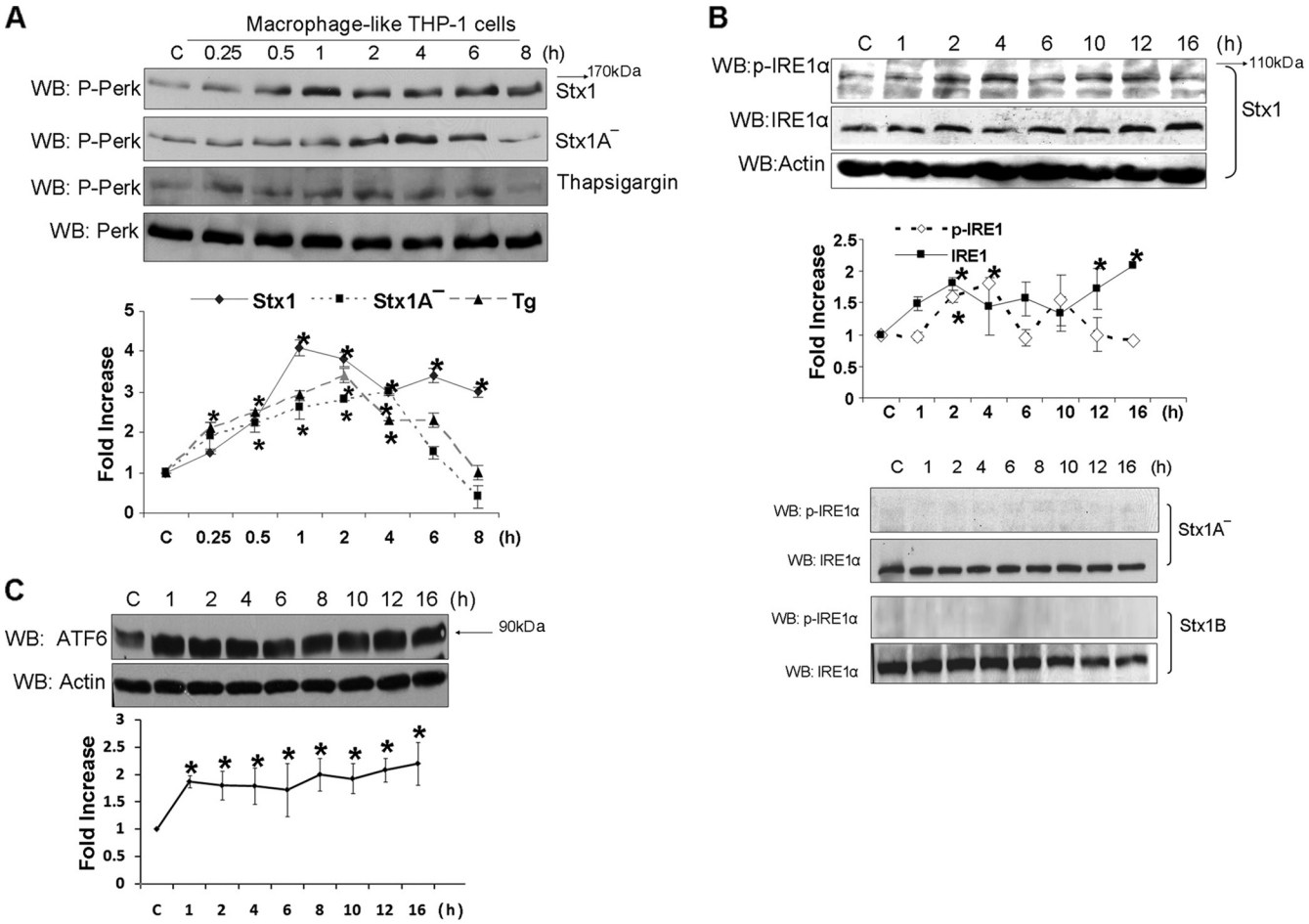


FIG. 1. Stx1 induces ER stress through the sensors PERK and IRE1α in human macrophage-like THP-1 cells. Differentiated, macrophage-like THP-1 cells ($1.0 \times 10^6$ cells/ml) were stimulated with Stx1, the enzymatic mutant Stx1A$^-$ (400 ng/ml), or Stx1 B-subunits (800 ng/ml). Tg (10 μM) was used as the positive control for activation of ER stress signaling. At the indicated times, cells were lysed, and the lysates were subjected to 8 to 12% SDS-PAGE followed by Western blotting (WB) using antibodies specific for the ER stress signaling molecules, including (A) PERK, (B) IRE1α, and (C) unprocessed 90-kDa ATF6. (Upper panels) Characteristic immunoblots; (lower panels) statistical analyses of densitometric scans from at least four independent experiments. The data are expressed as mean ± SEM increases in (A) phospho-PERK (P-PERK), (B) phospho-IRE1α (p-IRE1) and total IRE1α (IRE1α), and (C) total 90-kDa ATF6 levels compared to the levels in untreated control cells (C) and were normalized using total PERK or actin levels. Asterisks indicate significant differences ($P < 0.05$) compared to control cells.

ratories Inc., Burlingame, CA), and 4′,6′-diamidino-2-phenylindole (DAPI) (300 nM; Invitrogen) in blocking buffer were added together as a secondary antibody and nuclear staining dye, respectively. After incubation for 1 h, slides were mounted on Vectashield (Vector Laboratories Inc.), covered with glass coverslips, and examined with a Stallion digital imaging station (Carl Zeiss Microscopy, Gottingen, Germany). Quantification of Bax, Bak, and Bcl-2 mitochondrial translocation and nuclear fragmentation in confocal images was performed by counting at least 75 treated or untreated cells per well from five independent experiments. Cells were scored positive for mitochondrial translocation if there was yellow or orange in merged images. Fragmented nuclei were detected by punctate DAPI blue staining, and the results were normalized using the total number of DAPI-stained cells.

**Statistical analysis.** The data are reported below as means ± standard errors of the mean (SEM) for at least four independent experiments. Statistical analyses of data were performed with Excel (Microsoft, Redmond, WA). Student's *t* test was used to measure differences in samples. Depending on the assay, a *P* value of <0.05, <0.005, or <0.001 was considered significant.

## RESULTS

**Stx1 induces ER stress in macrophage-like THP-1 cells through activation of the sensor molecules PERK and IRE1α.** We previously demonstrated that Stx1 induced ER stress in monocytic THP-1 cells through the ER membrane-bound sensors PERK, IRE1α, and ATF6. Signaling through these molecules led to coordinate regulation of ER stress-associated target proteins and rapid onset of apoptosis (25). To assess the induction of ER stress in macrophage-like THP-1 cells, differentiated cells were stimulated from 0 to 8 h with purified Stx1 or Stx1 mutant holotoxin Stx1A$^-$ containing two point mutations that dramatically reduce the enzymatic activity and the ability to induce apoptosis. Tg, an irreversible inhibitor of the sarcoplasmic ER $Ca^{2+}$ ATPase, was used as a positive control for PERK activation. We observed persistent PERK activation when cells were treated with Stx1; the activation peaked at a 4.1-fold increase ($P < 0.05$) at 1 h and remained elevated (3.0-fold increase; $P < 0.05$) up to 8 h after treatment (Fig. 1A). Both Stx1A$^-$ and Tg mediated transient increases in PERK phosphorylation that progressively decreased 6 to 8 h after treatment. Consistent with these findings, we noted that treatment of cells with Stx1 resulted in prolonged activation of the

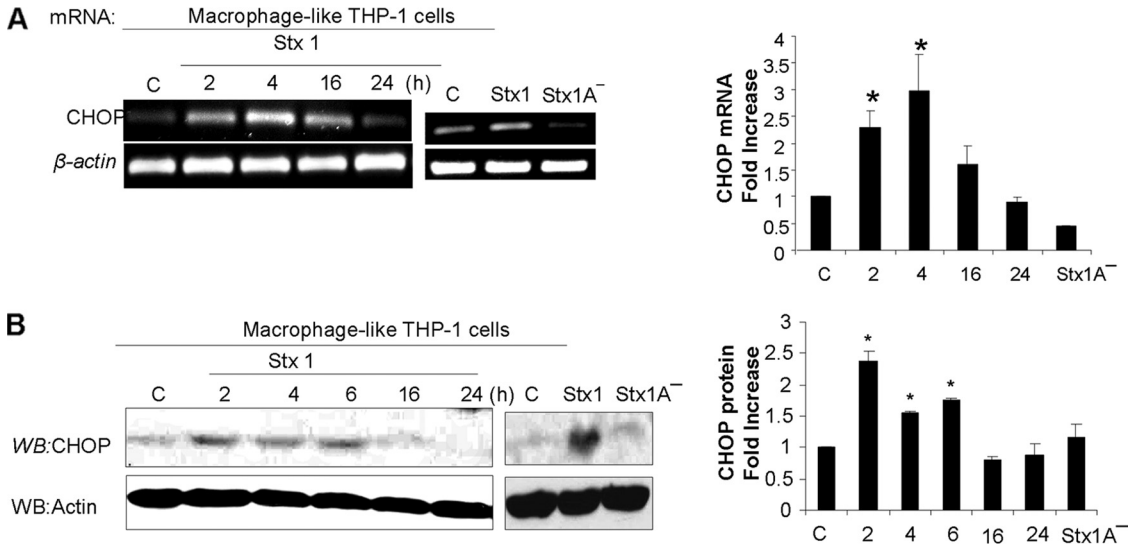


FIG. 2. Stx1 induces CHOP expression in THP-1 cells. (A) Macrophage-like THP-1 cells were treated with Stx1 for 0 to 24 h or with Stx1 or Stx1A$^-$ for 0 to 4 h. To measure changes in CHOP transcript levels, RT-PCR was performed as described in Materials and Methods. Resultant cDNAs were resolved on 1.5% agarose gels and visualized using ethidium bromide. (B) Macrophage-like THP-1 cells were treated with Stx1 for 0 to 24 h or with Stx1 or Stx1A$^-$ for 0 to 2 h. CHOP expression and β-actin protein expression following Stx1 treatment for the indicated times were determined by Western blotting (WB). The bar graphs show the results of statistical analyses of data from densitometric scans from four independent experiments, and the data are expressed as mean and SEM increases in CHOP mRNA or protein levels compared to the levels in untreated control cells (C) and were normalized using β-actin levels. Asterisks indicate significant differences ($P < 0.05$) compared to control cells.

PERK substrate eIF-2α (http://medicine.tamhsc.edu/basic-sciences/mmp/faculty/materials/tesh-bcl-2.html). At later time points, PERK activation and eIF-2α activation were maintained up to 16 h after Stx1 treatment (2.8-fold increase; $P < 0.05$) and returned to basal levels at 24 h. Stx1A$^-$ did not induce PERK or eIF-2α activation at later time points (data not shown). As was the case for monocytic THP-1 cells, Stx1 increased IRE1α release in soluble fractions of macrophage-like cells, which peaked at a 2.1-fold increase 16 h after toxin treatment (Fig. 1B). We also observed a transient increase in IRE1α phosphorylation at Ser$^{724}$, a well-described characteristic of the ER stress response. IRE1α phosphorylation remained at basal levels following Stx1A$^-$ and Stx1 B-subunit treatment (Fig. 1B, lower panel). Activation of the IRE1α endonuclease function by Stx1 treatment was shown by splicing of the XBP-1 transcript (http://medicine.tamhsc.edu/basic-sciences/mmp/faculty/materials/tesh-bcl-2.html). Interestingly, the total levels of XBP-1 transcripts were also increased 6 h after Stx1 treatment. In contrast to the findings for monocytic THP-1 cells, in which Stx1 treatment rapidly triggered ATF6 processing (25), we did not detect ATF6 proteolysis (loss of the 90-kDa unprocessed protein) after treatment of macrophage-like THP-1 cells with Stx1 (Fig. 1C). Slightly elevated levels of unprocessed ATF6 were detected by immunoblotting after toxin treatment. Collectively, these data suggest that, unlike for monocytic THP-1 cells, where Stx1 signals through all ER stress sensors, the toxin selectively activates the sensor molecules PERK and IRE1α, but not ATF6, in macrophage-like cells. Furthermore, toxin enzymatic activity appears to be necessary for prolonged sensor activation.

**Stx1 intoxication of THP-1 cells leads to increased expression of the ER stress target molecules CHOP and BiP.** The transcription factor CHOP and the ER resident chaperone BiP are regulated by ER stress signal transducers responding to unfolded proteins within the ER lumen (15, 22). We previously showed that CHOP mRNA expression and CHOP protein expression were upregulated in undifferentiated THP-1 cells following treatment with Stx1 over a 12-h period (25). Based on these previous data and our demonstration of PERK and IRE1α activation, we hypothesized that Stx1 activates CHOP expression in macrophage-like THP-1 cells. Cells were stimulated with Stx1 for 0 to 24 h, and CHOP transcript and protein levels were measured by RT-PCR and immunoblotting, respectively. Treatment of differentiated THP-1 cells with Stx1 induced CHOP transcript expression (Fig. 2A) and protein expression (Fig. 2B) that were elevated 2 to 4 h after treatment but decreased at later time points. Although capable of transient PERK activation, Stx1A$^-$ did not elicit CHOP mRNA or protein expression 4 h after treatment. At later time points, the Stx1A$^-$ holotoxin and Stx1 B-subunits caused increases in CHOP protein levels only at single time points (6 and 12 h, respectively); however, Stx1A$^-$ and Stx1 B-subunits did not trigger apoptosis (14). The sarcoplasmic ER $Ca^{2+}$ ATPase inhibitor Tg was a potent inducer of CHOP protein expression (data not shown).

Under normal homeostatic conditions, proximal sensors of unfolded proteins remain associated with chaperone proteins, such as BiP, at the ER membrane (2). In the presence of elevated levels of improperly folded proteins, chaperones dissociate from ER stress sensors and bind unfolded proteins. BiP dissociation from the sensors is thought to be crucial for sensor dimerization and activation. Given the evidence that Stxs bind to chaperones (12, 43) and activate the ER stress response, we reasoned that chaperone protein expression may be altered by Stx1 treatment. We treated monocytic and macrophage-like THP-1 cells with Stx1 or Tg for 0 to 120 min and then isolated

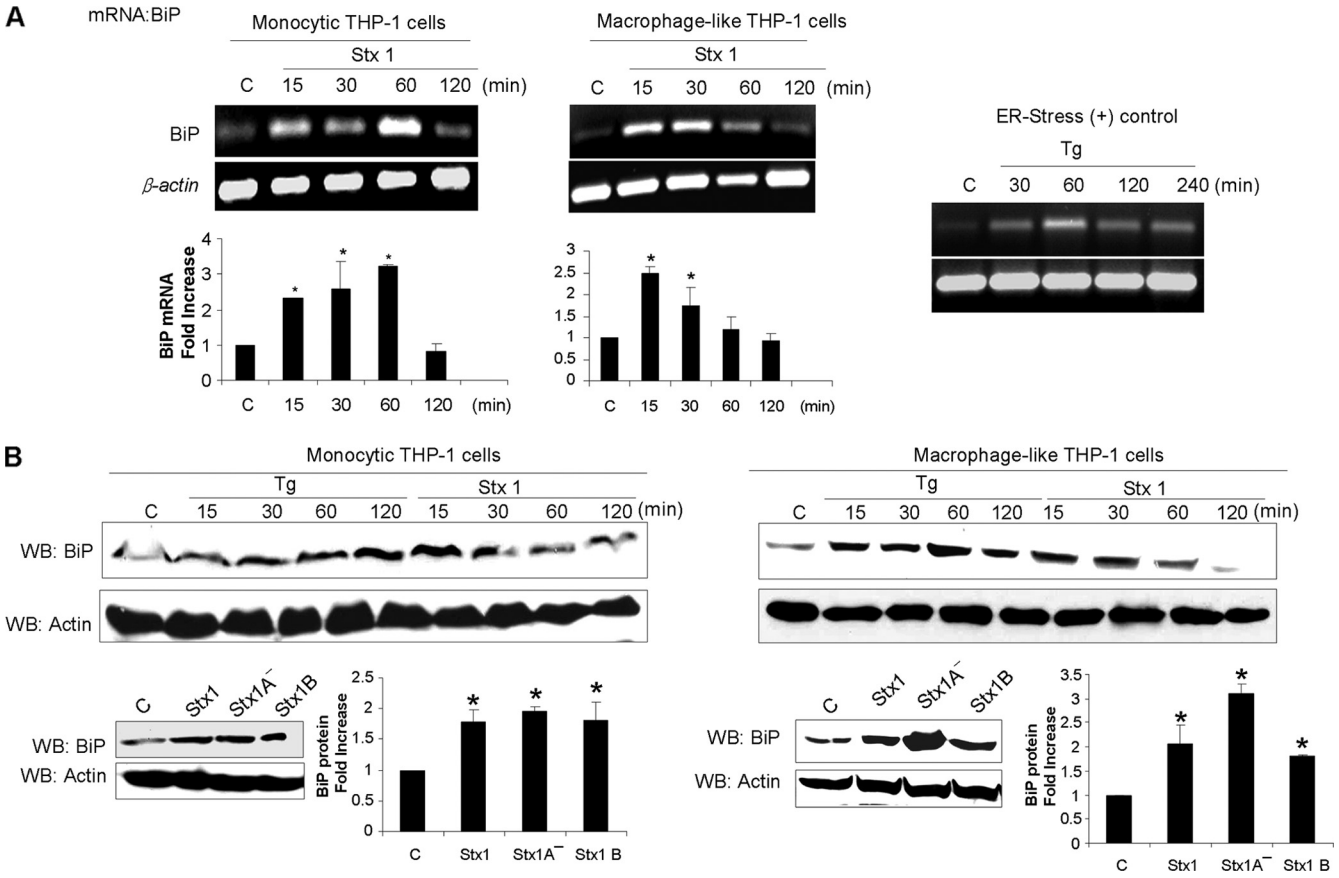


FIG. 3. Stx1 induces BiP expression in THP-1 cells. (A) Following treatment with Stx1 or Tg for the indicated times, total RNA was extracted from monocytic or macrophage-like THP-1 cells. RT-PCR using primers specific for BiP were used to assess BiP mRNA induction. (B) Following treatment with Stx1 or Tg for 0 to 2 h (upper panels) or treatment with Stx1, Stx1A$^-$, or purified Stx1 B-subunits (Stx1B) for 30 min (lower panels), cell lysates were prepared from monocytic or macrophage-like THP-1 cells. Equal amounts of proteins were subjected to Western blot (WB) analysis using antibodies specific for BiP or β-actin. The bar graphs show the results of statistical analyses of data derived from four independent experiments. The data are expressed as mean and SEM increases in BiP mRNA or protein levels compared to the levels in untreated control cells (C) and were normalized using β-actin levels. Asterisks indicate significant differences ($P < 0.05$) compared to control cells.

total RNA for RT-PCR quantitation of BiP mRNA expression or prepared cell lysates for immunoblotting. Stx1-induced ER stress led to rapid (within 15 min) increases in BiP mRNA levels, which declined at 120 min after toxin treatment in both monocytic and macrophage-like THP-1 cells (Fig. 3A). BiP protein levels in Stx1-treated cells were correlated with mRNA results, showing that there was increased BiP expression within 15 min after toxin treatment (Fig. 3B). To examine the roles of toxin enzymatic activity and B-subunit retrograde transport in increased BiP expression, we treated monocytic and macrophage-like THP-1 cells with Stx1, Stx1A$^-$, or purified Stx1 B-subunits for 30 min. Cell lysates were prepared, and equal concentrations of proteins were transferred to membranes for probing with anti-BiP antibodies. All of the Stx1 treatments induced higher levels of BiP expression compared to the results for untreated control cells (Fig. 3B, lower panels). These data suggest that following retrograde transport to the ER, individual toxin subunits may be "sensed" as misfolded proteins, leading to increased expression or stabilization of the chaperone BiP. In contrast, activation of the transcription factor CHOP appears to require enzymatic activity.

**Stx1 transiently increases Bax and Bak expression and induces translocation of these molecules to mitochondria in THP-1 cells.** Stx1 induces the release of $Ca^{2+}$ from ER stores in THP-1 cells (6, 25). In response to elevated levels of misfolded proteins in the ER, the BH1-3-containing proapoptotic proteins Bax and Bak associate with the ER membrane to create $Ca^{2+}$-specific pores. The efflux of $Ca^{2+}$ from ER stores contributes to activation of the intrinsic apoptotic pathway. Thus, maintenance of $Ca^{2+}$ homeostasis is a control factor in apoptosis (36). ER stress-activated release of $Ca^{2+}$ from ER stores may induce apoptosis in part through transcriptional and translational activation of Bax and Bak expression. Therefore, we determined whether Stx1 induced the expression of Bax and Bak mRNA and proteins in monocytic and macrophage-like THP-1 cells. Characteristic immunoblots are shown in Fig. 4A, while the results of statistical analyses of data derived from four independent experiments are shown in the bar graphs. Increased expression of the Bax and Bak proteins was detected 15 min after Stx1 treatment of monocytic cells, and the expression of these proteins peaked at 15 min (3.3-fold; $P < 0.005$) and 30 min (2.3-fold; $P < 0.05$), respectively.

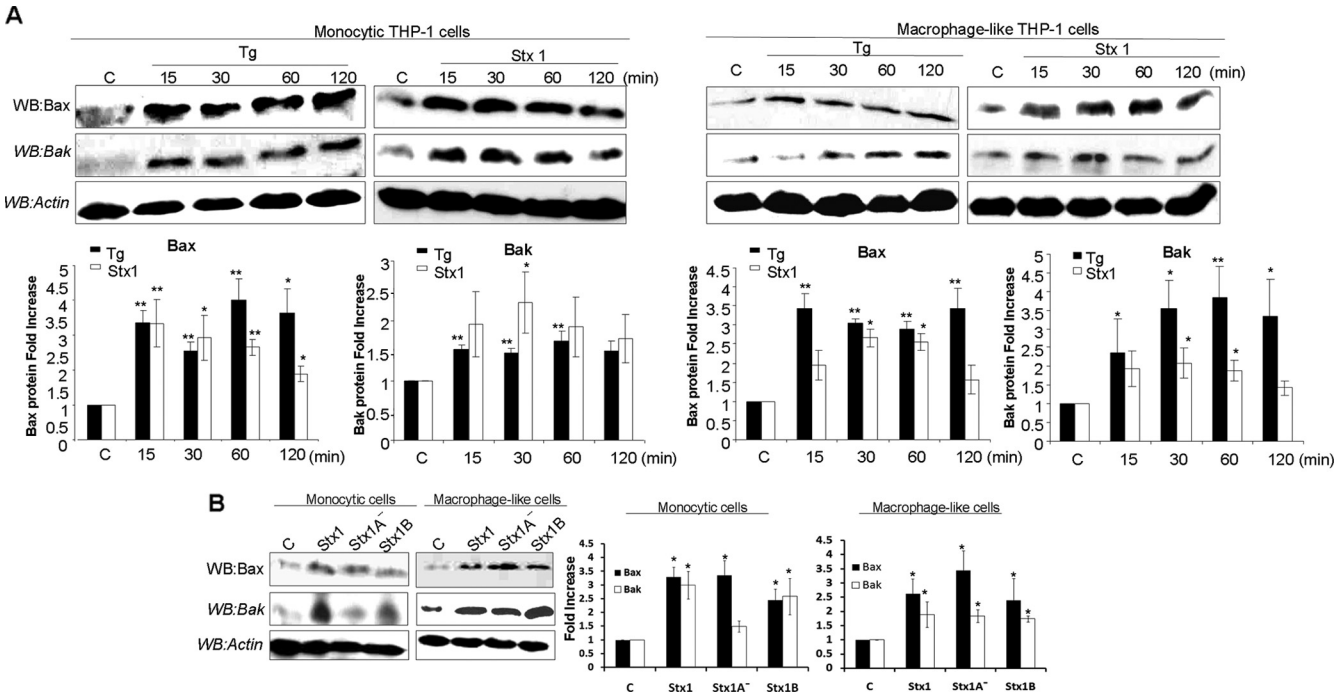


FIG. 4. Stx1 induces transient expression of the proapoptotic factors Bax and Bak in THP-1 cells. (A) Monocytic and macrophage-like THP-1 cells were treated with Stx1 or the ER stress inducer Tg for the indicated times. Cell lysates were prepared, and equal amounts of protein were subjected to Western blot (WB) analysis for Bax, Bak, and actin expression. Characteristic immunoblots are shown in the upper panels. (B) Monocytic and macrophage-like THP-1 cells were treated with Stx1, Stx1A$^-$, or Stx1 B-subunits for 30 min, and Bax, Bak, and actin expression was determined by Western blotting (WB). The bar graphs show the results of statistical analyses of data derived from five independent experiments. The data are expressed as mean ± SEM increases in Bax or Bak expression compared to the expression in untreated control cells (C) and were normalized using actin expression. Asterisks indicate significant differences (*, $P < 0.05$; **, $P < 0.005$) compared to control cells.

Stx1 also increased Bax and Bak expression in macrophage-like cells, although the induction kinetics were delayed compared to those in monocytic cells. Elevated levels of Bax and Bak protein expression were observed with Stx1, Stx1A$^-$, or Stx1 B-subunit treatment after 30 min (Fig. 4B), suggesting that toxin enzymatic activity is not required for increased expression. Stx1 treatment was associated with rapid induction of *bax* transcripts in the monocytic THP-1 cells (4.4-fold increase, peaking at 15 min; $P < 0.001$), while increases in *bax* mRNA levels in macrophage-like cells were slightly delayed (2-fold increase, peaking at 30 min; $P < 0.05$) (http://medicine.tamhsc.edu/basic-sciences/mmp/faculty/materials/tesh-bcl-2.html).

Bax and Bak translocation and association with the mitochondrial membrane trigger the intrinsic pathway of apoptosis (28, 33). To study the involvement of Stx1 in triggering mitochondrial translocation of Bax, we performed confocal fluorescence microscopy with Stx1-treated monocytic and macrophage-like THP-1 cells using fluorescein isothiocyanate-conjugated anti-Bax antibody and MitoTracker Red (Fig. 5A). Bax rapidly translocated to mitochondria of monocytic cells, and 33% of the cells ($P < 0.001$) showed punctuate yellow fluorescence in merged images 15 min after toxin treatment. There was extensive nuclear fragmentation in Stx1-treated monocytic cells at 4 h, suggesting that there was rapid apoptosis following intoxication. Bax translocation was delayed in macrophage-like cells, and 22% of the total cells ($P < 0.01$) showed evidence of Bax association with mitochondria 60 min after intoxication. Nuclear fragmentation was not observed following short-term treatment of macrophage-like cells with Stx1. In contrast to the results for Stx1 treatment, Bax mitochondrial translocation and nuclear fragmentation were not observed after Stx1A$^-$ holotoxin or Stx1 B-subunit treatment for 4 h, suggesting that Stx1 enzymatic activity is required to relay signals to induce apoptosis (Fig. 5A). We observed mitochondrial translocation of Bak in macrophage-like cells treated with Stx1 for 1 h (Fig. 5B). Quantitative analysis showed that the number of cells with translocated Bak was significantly greater for Stx1-treated cells (34.3% of total cells; $P < 0.001$) than for control cells. Stx1A$^-$ and Stx1 B-subunits did not induce Bak mitochondrial translocation (data not shown). Tg was used as a positive control for confocal imaging of Bax and Bak translocation (data not shown).

**Stx1 induces expression of the antiapoptotic factor Bcl-2, which associates with mitochondria in macrophage-like cells.** Our observation that the onset of apoptosis mediated by Stx1 in macrophages is delayed compared to that in monocytic cells suggested that Stx1 triggers alternative signaling pathways in differentiated cells responsible for the transient survival phenotype. One possible explanation for the longer life span of macrophage-like THP-1 cells following intoxication may be expression of antiapoptotic members of the Bcl-2 family of apoptosis regulators. We previously observed decreased levels of Bcl-2 transcripts beginning 2 h after toxin treatment of monocytic THP-1 cells (25). To address whether changes in Bcl-2 expression are correlated with cell survival following toxin challenge, Bcl-2 and Bcl-xL mRNA and protein levels

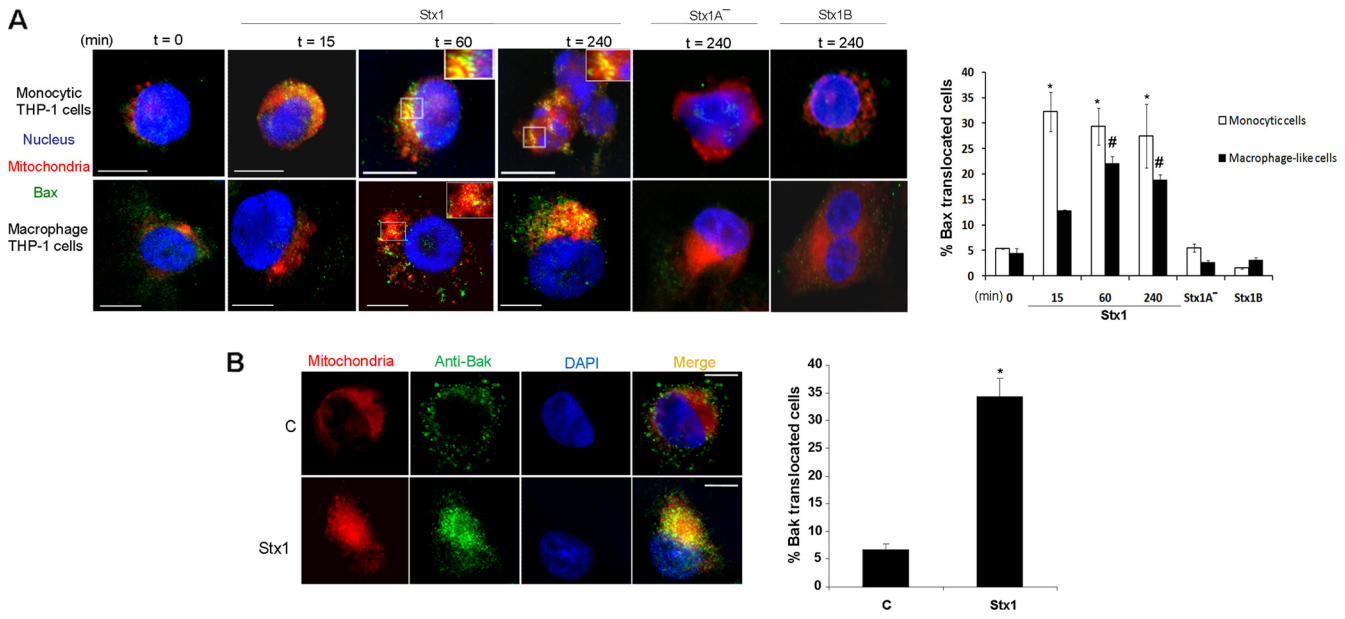


FIG. 5. Mitochondrial translocation of Bax and Bak in Stx1-treated THP-1 cells. (A) Monocytic (upper panels) and macrophage-like (lower panels) THP-1 cells were treated or not treated with Stx1 (400 ng/ml), Stx1A$^-$ (400 ng/ml), or Stx1 B-subunits (800 ng/ml) for the indicated times. Cells were treated with 300 nM Mitotracker Red for detection of mitochondria, fixed, permeabilized, and stained with anti-Bax primary antibodies for 2 h at 37°C. After washing, cells were stained with secondary fluorescein-conjugated antibody for Bax detection (green) and DAPI (blue) for nuclear staining. After mounting, cells were visualized by confocal laser microscopy. Note the colocalization of Bax with mitochondria in merged images. Increased resolution of merged images is shown in the insets. Scale bars = 10 μm; original magnification, ×63. (B) Differentiated THP-1 cells ($5 \times 10^5$ cells/ml) were plated on eight-well chamber slides and stimulated with Stx1 (400 ng/ml) for 1 h. The method described above was used for confocal microscopy, except that anti-Bak as used as the primary antibody. For quantitative analyses of confocal images, cells with evidence of Bax or Bak mitochondrial translocation (orange or yellow in merged images) were counted for each treatment and scored for four independent experiments. The bar graphs show the percentages (means ± SEM) of cells with Bax or Bak translocation normalized to the total cell number. Statistical significance (#, $P < 0.01$; *, $P < 0.001$) was assessed by comparing control (C) and Stx1 treatments.

were analyzed at various times after treatment of macrophage-like cells with Stx1. Stx1 treatment increased Bcl-2 mRNA expression, which peaked at 2 to 4 h after toxin exposure and declined to levels near control levels in 24 h (Fig. 6A), and it also increased Bcl-2 protein expression, which remained elevated for 12 h after toxin treatment (Fig. 6B). To examine whether enzymatic activity or purified B-subunits affect anti-apoptotic signaling, macrophage-like cells were exposed to Stx1, Stx1A$^-$ holotoxin, or Stx1 B-subunits for 6 or 12 h, which was followed by Western blotting to measure Bcl-2 expression (Fig. 6C). Bcl-2 induction was observed with all treatments, suggesting that enzymatic activity is not required and B-subunit retrograde transport is sufficient for Bcl-2 induction. Stx1 did not appear to alter expression of the Bcl-xL protein in either monocytic or macrophage-like THP-1 cells (Fig. 6D). Thus, in contrast to monocytic THP-1 cells, which downregulate expression of the antiapoptotic factor Bcl-2 and undergo rapid cell death, macrophage-like cells persistently express Bcl-2, which may initially counterbalance apoptotic signaling triggered by Stx1.

The prosurvival functions of Bcl-2 remain to be fully characterized, but they may involve association of Bcl-2 with pro-apoptotic members of the Bcl-2 family of proteins, such as Bax and Bak, at the mitochondrial membrane, which blocks cytochrome *c* release and subsequent formation of the apoptosome (7, 16). Confocal microscopy with fluorescein isothiocyanate-labeled (green) anti-Bcl-2 antibodies and MitoTracker Red was employed to examine the subcellular localization of Bcl-2 following treatment of monocytic and macrophage-like THP-1 cells with Stx1 for 4 h and 12 h (Fig. 7A). In monocytic cells, the overall Bcl-2-associated fluorescence was reduced by toxin treatment compared to that in control cells, and significantly reduced numbers of cells showed Bcl-2 colocalization with mitochondria (Fig. 7B). In macrophage-like cells, the Bcl-2 signal did not diminish over time, and colocalization of Bcl-2 with mitochondria was evident in merged images. Again, we noted extensive nuclear fragmentation and cell shrinkage in monocytic cells, while nuclei of macrophage-like THP-1 cells were not as severely damaged (Fig. 7C).

**Stx 1 induces differential phosphorylation of Bcl-2 in monocytic and macrophage-like THP-1 cells.** Stx1 has been shown to trigger the stress-activated JNK and p38 mitogen-activated protein kinase (MAPK) cascades in many types of cells (5, 17, 37), and the activation of apoptotic and survival signaling by Stx1 in macrophage-like THP-1 cells is associated with prolonged activation of JNK and p38 MAPKs (24). Ito et al. (18) noted that phosphorylation of Bcl-2 at Ser$^{70}$ may be required for full and potent antiapoptotic activity. However, alternative phosphorylation of Bcl-2 by p38 MAPK, particularly at Thr$^{56}$, was reported to inhibit antiapoptotic activity (8). We therefore examined the phosphorylation status of Bcl-2 in monocytic and macrophage-like THP-1 cells treated with Stx1 (Fig. 8). Stx1 treatment of monocytic cells was associated with the loss of Ser$^{70}$-phospho-Bcl-2 and Thr$^{56}$-phospho-Bcl-2 6 h after toxin exposure, a time at which a significant fraction of monocytic cells were apoptotic. In macrophage-like cells, the levels of

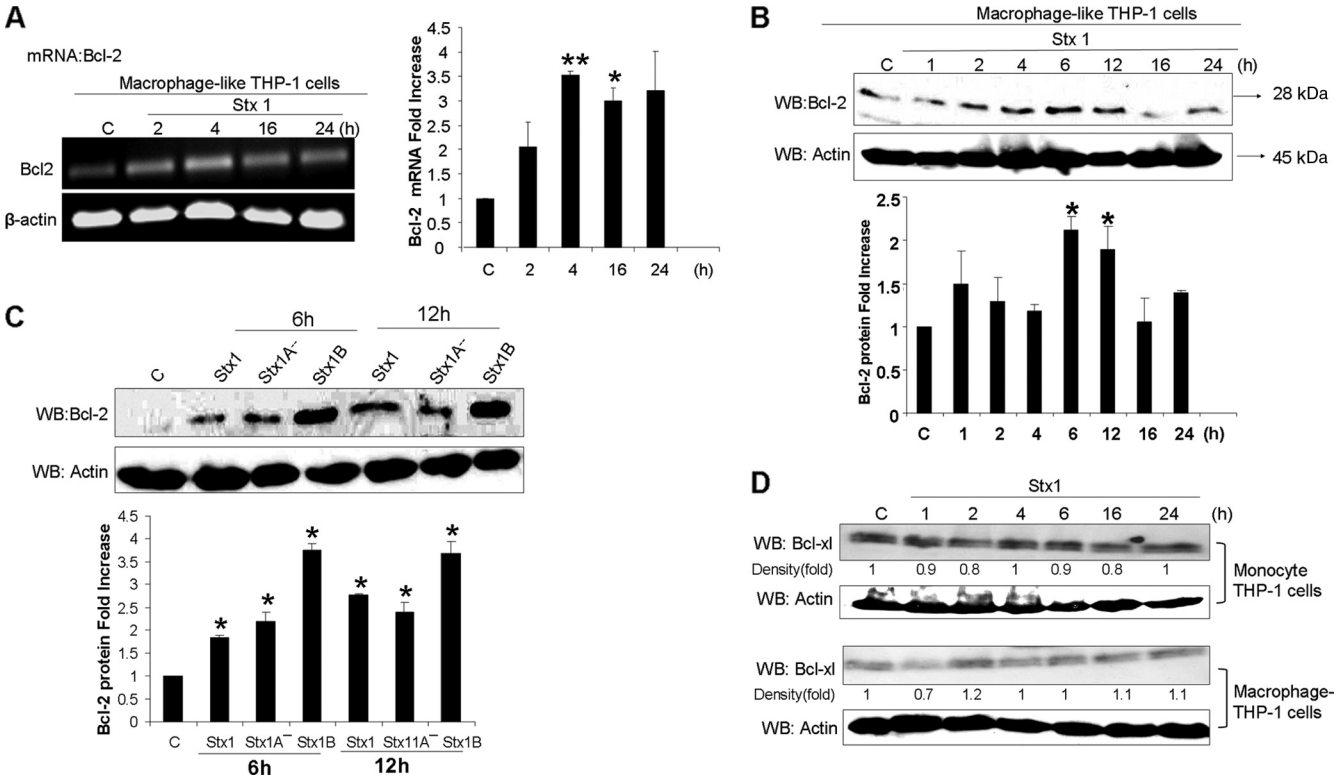


FIG. 6. Induction of antiapoptotic factors Bcl-2 and Bcl-xL in Stx1-treated macrophage-like THP-1 cells. (A) THP-1 cells were not treated or treated with Stx1 (400 ng/ml), and at the indicated time points total RNA was isolated to perform RT-PCR using a specific primer set for *bcl-2* transcript analysis. β-Actin mRNA expression was measured as an internal control under the same conditions that were used for *bcl-2* mRNA induction. (B) THP-1 cells were treated with Stx1 for the indicated times. Cell lysates were prepared, and equal amounts of protein were subjected to Western blot (WB) analysis for Bcl-2 and actin expression. (C) THP-1 cells were not treated or treated with Stx1, Stx1 $A^-$, or Stx1 B-subunits, and at the indicated times cell lysates were prepared. Equal amounts of protein were subjected to Western blot (WB) analysis for Bcl-2 expression. The bar graphs in panels A to C show the results of statistical analyses of data derived from four independent experiments. The data are expressed as mean and SEM increases in Bcl-2 expression compared to the expression in untreated control cells (C) and were normalized using actin expression. Asterisks indicate significant differences (*, $P < 0.05$; **, $P < 0.001$) compared to control cells. (D) Bcl-xL protein expression levels were determined by Western blot analysis using anti-human Bcl-xL monoclonal antibodies. Band intensities were measured by densitometry, and changes are indicated below the lanes. Actin protein levels were used as equal protein loading controls. The results shown are representative of the results of four independent experiments.

$Ser^{70}$-phospho-Bcl-2 and $Thr^{56}$-phospho-Bcl-2 in untreated (control) cells were dramatically reduced compared to the levels in control monocytic cells. However, the phosphorylation of Bcl-2 at $Ser^{70}$ was significantly increased compared with that in control cells after treatment with Stx1 for 1 and 2 h (2.8-fold increase [$P < 0.05$] and 4-fold increase [$P < 0.05$], respectively). $Thr^{56}$-phospho-Bcl-2 was not detectable throughout the time course of the experiment. Thus, Stx1 differentially regulates Bcl-2 phosphorylation events in THP-1 cells in a cell maturation-dependent manner. Monocytic cells maintain expression of the attenuated form of Bcl-2. Differentiated cells dramatically upregulate phosphorylation of the antiapoptotic form of the molecule, while the inactive form of Bcl-2 is undetectable.

## DISCUSSION

We have shown that Stx1, a bacterial toxin routed to the ER, induces apoptosis in the human myeloid cell line THP-1 in a cell maturation-dependent manner. Monocytic cells were rapidly killed by this toxin through mechanisms involving (i) the activation of ER stress sensors; (ii) the release of $Ca^{2+}$ from ER stores, leading to calpain activation and proteolysis of procaspase-8; and (iii) the production of TRAIL and DR5, leading to caspase-8 activation. In contrast, macrophage-like THP-1 cells displayed delayed apoptosis when they were treated with Stx1, which was accompanied by transient increases in total protein synthesis and cytokine and chemokine production (14, 23). We show here that cell maturation is associated with changes in the ER stress response, leading to activation of proapoptotic and counterbalancing prosurvival signals. A comparison of the signaling pathways activated by Stx1 in monocytic and macrophage-like THP-1 cells is shown in Table 1. While all three proximal ER stress sensors were activated in monocytic cells, Stx1 activated PERK and IRE1α, as well as their downstream substrates eIF-2α and XBP-1, in macrophage-like cells. Thus, differentiation appeared to be associated with the loss of proteolysis and signaling through the bZIP transcription factor ATF6. In response to ER stress, membrane-bound ATF6 is cleaved by site 1 and site 2 proteases that separate the active transcription factor from the transmembrane domain. Activated ATF6 binds to promoters

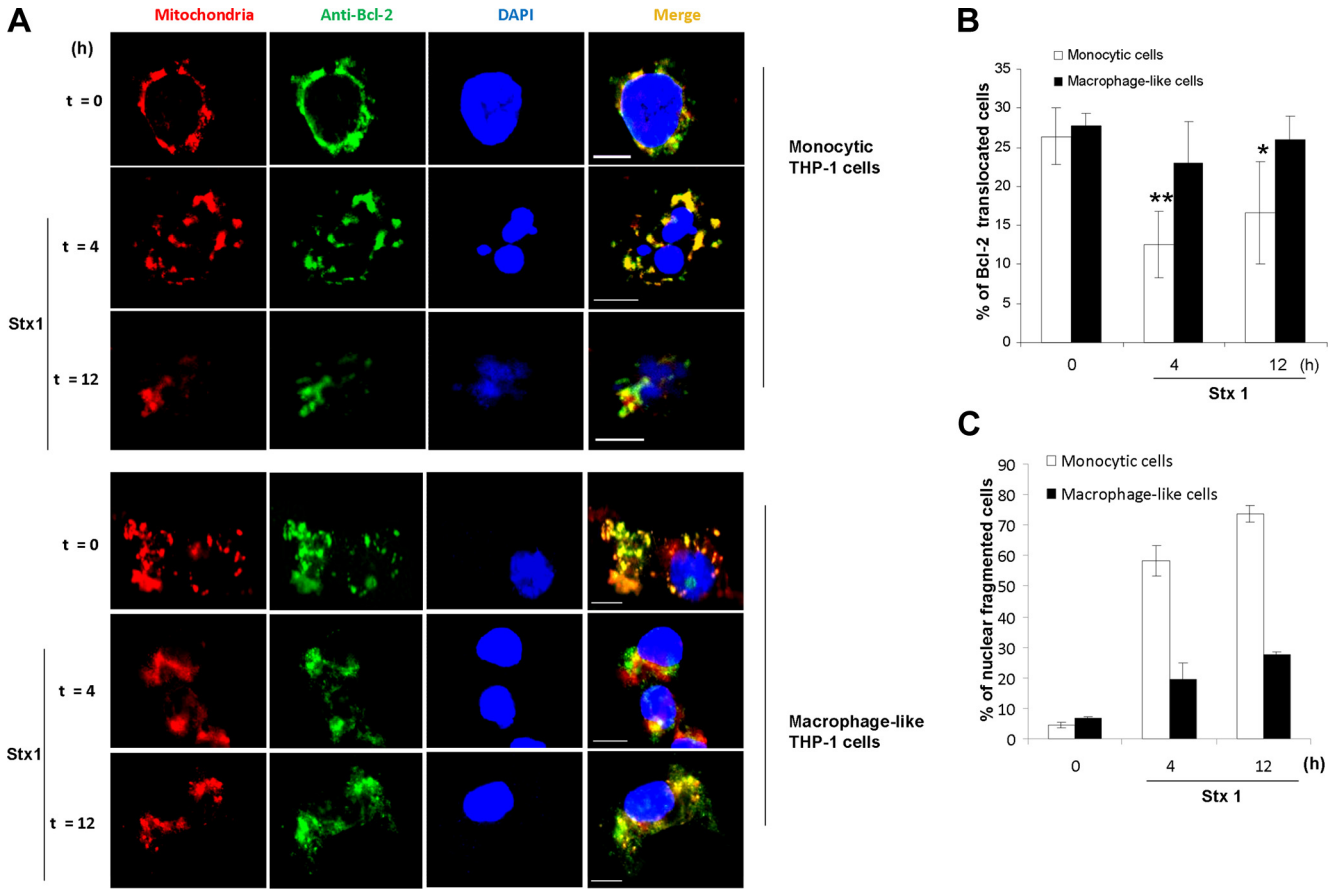


FIG. 7. Mitochondrial translocation of Bcl-2 in Stx1-treated THP-1 cells. (A) Monocytic and macrophage-like THP-1 cells were treated with or without Stx1 for 4 h or 12 h. Cells were treated with 300 nM Mitotracker Red for detection of mitochondria, fixed, permeabilized, and stained with anti-Bcl-2 primary antibodies. After washing, cells were stained with secondary fluorescein-conjugated antibody for Bcl-2 detection (green) and with DAPI (blue) for nuclear staining. After mounting, cells were visualized by confocal laser microscopy. Note the extensive nuclear fragmentation and lack of Bcl-2 colocalization with mitochondria in Stx1-treated monocytic cells. In toxin-treated macrophage-like cells, note the colocalization of Bcl-2 with the nucleus and mitochondria in the merged image. For quantitative analyses of confocal images, cells with evidence of Bcl-2 mitochondrial translocation (orange or yellow in merged images) or nuclear fragmentation were counted for each treatment and scored for four independent experiments. The bar graphs show the mean ± SEM percentages of cells with (B) Bcl-2 translocation or (C) nuclear fragmentation normalized using the total cell number. The statistical significance of Bcl-2 translocation was assessed by comparing control and Stx1 treatments (*, $P < 0.05$; **, $P < 0.001$). Scale bar = 10 μm; original magnification, ×63.

containing ER stress elements (ERSE), which are complex *cis*-active promoter elements that also contain binding sites for CBF/NF-Y and TATA-binding protein (27, 42). Many ER stress-regulated genes, including those encoding BiP and CHOP, contain ERSE, and we have shown that both BiP expression and CHOP expression are increased by Stx1 treatment of monocytic and macrophage-like THP-1 cells. How does Stx1 induce the increased expression of BiP and CHOP in macrophage-like cells in the absence of ATF6 activation? Previous studies have shown that the endonuclease function of IRE1α splices the XBP-1 transcript to form the active transcription factor, and activated XBP-1 may also bind to ERSE in a CBF/NF-Y-dependent manner. Thus, redundant signaling functions of IRE1α appear to be capable of compensating for the loss of ATF6 activation.

In a previous study using monocytic THP-1 cells, we noted that the Stx1A$^-$ holotoxin failed to activate PERK and ATF6 in monocytic cells (25). In the present study, we showed that Stx1A$^-$ transiently activates PERK and does not activate IRE1α in macrophage-like cells. Stx1A$^-$ and purified Stx1 B-subunits were capable of signaling increased BiP expression, but the enzymatic mutant did not elicit persistent increases in CHOP expression in monocytic (25) or macrophage-like THP-1 cells. Since the E167Q R170L double mutation in Stx1A$^-$ holotoxin conferred a >5-log reduction in Vero cell toxicity (31), it is unlikely that the transient PERK activation and increased BiP expression were due to residual enzymatic activity. These data suggest that the introduction of Stx1, Stx1A$^-$ holotoxin, or Stx1 B-subunits into the ER lumen per se may be sufficient to trigger ER stress leading to association of chaperone proteins with the toxins and ER stress sensor activation for increased BiP expression. However, Stx1A$^-$ holotoxin and Stx1 B-subunits do not trigger programmed cell death. Prolonged CHOP expression, which has been associated with induction of apoptosis in vitro and in vivo (13, 38), may require toxin enzymatic activity. Thus, ongoing generation of truncated and/or misfolded host proteins may be necessary for signaling leading to apoptosis. These studies focused on the

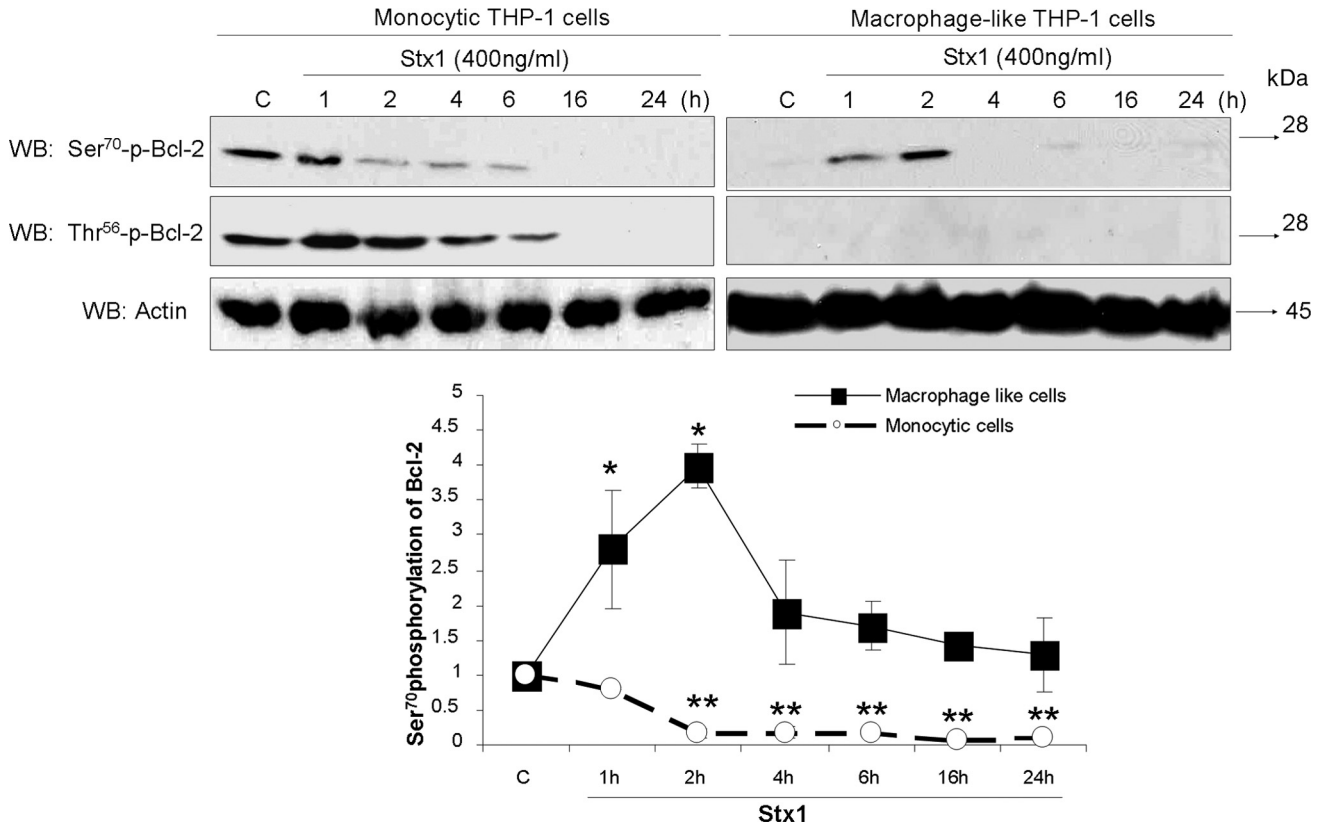


FIG. 8. Effect of Stx 1 on site-specific Bcl-2 phosphorylation in THP-1 cells. Monocytic and macrophage-like THP-1 cells were stimulated with Stx1 for the indicated time periods. Cell extracts containing 100 μg of protein were subjected to Western blot (WB) analysis to measure levels of expression of Bcl-2 phosphorylated at $Ser^{70}$ or $Thr^{56}$. Detection of actin levels served as a loading control. Mean ± SEM changes in $Ser^{70}$-phospho-Bcl-2 levels compared to the levels in untreated control cells from at least four independent experiments are shown in the lower panel. Asterisks indicate significant differences (*, $P < 0.05$; **, $P < 0.01$) compared to control cells (C).

response of human macrophage-like cells to Stx1. However, epidemiological studies have indicated that infection with Stx2-producing *E. coli* is more likely to progress to life-threatening extraintestinal complications such as hemolytic-uremic syndrome (for a review, see reference 40), and use of purified toxins in animal models revealed that Stx2 is more toxic (41). Therefore, comparative studies of ER stress and induction of apoptosis by Stx1 and Stx2 are in progress.

Members of the Bcl-2 family regulate the release of cytochrome *c* from mitochondria. The proapoptotic Bcl-2 proteins Bax and Bak form channels within the mitochondrial outer membrane that disrupt the membrane potential, resulting in cytochrome *c* release. Stx1 triggered a rapid, transient increase in the level of *bax* and *bak* mRNA, which peaked at 30 min after treatment of monocytic and macrophage-like THP-1 cells. The Bax and Bak protein levels also increased in both types of cells. Confocal microscopy studies showed that Bax rapidly translocated to the mitochondria following toxin treatment of the cells. Bcl-2 and Bcl-xL possess antiapoptotic functions that may act by blocking the mitochondrial outer membrane permeabilization caused by the proapoptotic Bcl-2 family members Bax and Bak (7). $Stx1A^-$ holotoxin and Stx1

TABLE 1. Signaling pathways activated by Stx1 in monocytic and macrophage-like THP-1 cells

| Cells | Estimated time to reach 50% apoptosis with Stx1 (h)[a] | Activation of ER stress sensors | | | Expression of ER stress effectors | | Expression of proapoptotic factors Bax and Bak | Bax and Bak mitochondrial translocation | Expression of prosurvival factors | | Bcl-2 phosphorylation | |
|---|---|---|---|---|---|---|---|---|---|---|---|---|
| | | PERK | Ire1α | ATF6 | CHOP | BiP | | | Bcl-2 | Bcl-xL | $Ser^{70}$-phospho-Bcl-2 | $Thr^{56}$-phospho-Bcl-2 |
| Monocytic THP-1 | 5 | +[b] | +[b] | +[b] | +[b] | + | ↑ (transient) | + | ↓[b] | −[c] | ↓ | −[c] |
| Macrophage-like THP-1 | 24 | + | + | − | + | + | ↑ (transient) | + | ↑ | −[c] | ↑ | ND[d] |

[a] Data from reference 14.
[b] Data from reference 25.
[c] No change detected.
[d] ND, not detected.

B-subunit signals increased Bax and Bak expression and triggered release of $Ca^{2+}$ from ER stores in monocytic and macrophage-like THP-1 cells (6, 25). Increased Bax and Bak expression potentiates $Ca^{2+}$ release from ER stores (39). However, treatment with the enzymatically deficient Stx1A$^-$ holotoxin and Stx1 B-subunits was not sufficient to cause mitochondrial translocation of proapoptotic factors, despite elevation of Bax and Bak expression. Thus, $Ca^{2+}$ release triggered by Stx1 A$^-$ or Stx1 B-subunits may not contribute to apoptosis and not activate the mitochondrial or intrinsic pathway.

The major difference that we have observed between the Stx1-induced ER stress response in monocytic cells and the Stx1-induced ER stress response in macrophage-like cells involves the antiapoptotic protein Bcl-2. Bcl-2 transcript expression was downregulated within 4 h of Stx1 treatment of monocytic cells (25), while the Bcl-2 transcript levels increased and peaked 4 h after toxin treatment in macrophage-like cells. Increases in transcript levels correlated with increased Bcl-2 protein levels that were maintained for up to 12 h after toxin treatment. This differential response was specific to Bcl-2 as the levels of Bcl-xL, another antiapoptotic member of the Bcl-2 family, were not altered by Stx treatment in monocytic and macrophage-like cells. In addition to quantitative changes in Bcl-2 protein levels, we observed differences in Bcl-2 protein translocation in the two differentiation states. In monocytic cells, Bcl-2 proteins remained in a punctate pattern and did not colocalize with mitochondria following toxin treatment. We also observed significant nuclear fragmentation in monocytic cells 4 h after toxin treatment. In contrast, Bcl-2 rapidly colocalized with mitochondria and nuclei following intoxication of macrophage-like cells, and we did not detect extensive changes in nuclear morphology after toxin exposure. Signaling through the MAPK ERK1/2 or JNK, resulting in phosphorylation of Bcl-2 at $Ser^{70}$ and other serine and threonine residues, appears to be necessary for the antiapoptotic function (9, 18). Specifically, phosphorylation of Bcl-2 at $Ser^{70}$ appears to facilitate Bcl-2 dimerization or Bcl-2–Bcl-xL heterodimerization (29). Recently, evidence was presented that p38 MAPK-dependent phosphorylation of Bcl-2 at $Thr^{56}$ and $Ser^{87}$ induced conformational changes that reduced the antiapoptotic potential (8). Thus, alternative phosphorylation states appear to be critical in posttranslational regulation of Bcl-2 function. We observed differential Bcl-2 phosphorylation patterns in Stx1-treated THP-1 cells. Control monocytic cells expressed Bcl-2 proteins phosphorylated at $Ser^{70}$ and $Thr^{56}$. The $Ser^{70}$- and $Thr^{56}$-phospho-Bcl-2 levels decreased rapidly in Stx1-treated monocytic cells. In contrast, $Ser^{70}$-phospho-Bcl-2 levels were upregulated in Stx1-treated macrophage-like cells, and expression was maintained for up to 16 h. $Thr^{56}$-phospho-Bcl-2 was undetectable in control macrophage-like cells, and its expression was not induced by Stx1. Collectively, the data suggest that the delayed apoptosis phenotype in Stx1-treated macrophage-like cells was associated with activation of prosurvival signaling, increased expression of Bcl-2, translocation of the protein to the mitochondria, and changes in Bcl-2 phosphorylation status such that Bcl-2 phosphorylation at position 70 is increased and prolonged.

In summary, we have shown that myeloid cells respond to Stx1 in vitro in a cell maturation-dependent manner. Monocytic THP-1 cells undergo rapid apoptosis without the production of soluble cytokines. Toxin treatment of differentiated cells is associated with cytokine production and delayed onset of apoptosis. Rapid apoptosis in monocytic cells is associated with robust activation of all ER stress sensors, leading to increased expression of CHOP, TRAIL, and DR5, decreased expression of the Bcl-2 protein, and loss of $Ser^{70}$-phospho-Bcl-2. Delayed onset of cell death in macrophage-like cells was associated with loss of signaling through ATF6, increased expression of CHOP and Bcl-2, and increased expression of $Ser^{70}$-phospho-Bcl-2 with a concomitant loss of $Thr^{56}$-phospho-Bcl-2. Collectively, these data suggest that Bcl-2 protects macrophage-like cells from rapid apoptosis induced by Stxs.

## ACKNOWLEDGMENTS

We thank Shinji Yamasaki and Cheleste Thorpe for gifts of reagents necessary to carry out the experiments and Rola Barhoumi for assistance with confocal microscopy. We thank Nick Pace, Jim Samuel, and Jon Skare for their careful reading of the manuscript.

This work was supported by Public Health Service grant RO1 AI34530 from the National Institute of Allergy and Infectious Diseases, National Institutes of Health (V.L.T.).

## REFERENCES

1. **Bernales, S., F. R. Papa, and P. Walter.** 2006. Intracellular signaling by the unfolded protein response. Annu. Rev. Cell Dev. Biol. **22:**487–508.
2. **Bertolotti, A., Y. Zhang, L. M. Hendershot, H. P. Harding, and D. Ron.** 2000. Dynamic interaction of BiP and ER stress transducers in the unfolded-protein response. Nat. Cell Biol. **2:**326–332.
3. **Breckenridge, D. G., M. Germain, J. P. Mathai, M. Nguyen, and G. C. Shore.** 2003. Regulation of apoptosis by endoplasmic reticulum pathways. Oncogene **22:**8608–8618.
4. **Cherla, R. P., S.-Y. Lee, and V. L. Tesh.** 2003. Shiga toxins and apoptosis. FEMS Microbiol. Lett. **228:**159–166.
5. **Cherla, R. P., S.-Y. Lee, P. L. Mees, and V. L. Tesh.** 2006. Shiga toxin 1-induced cytokine production is mediated by MAP kinase pathways and translation initiation factor eIF4E in the macrophage-like THP-1 cell line. J. Leukoc. Biol. **79:**397–407.
6. **Cherla, R. P., S.-Y. Lee, R. A. Mulder, M.-S. Lee, and V. L. Tesh.** 2009. Shiga toxin 1-induced proinflammatory cytokine production is regulated by the phosphotidylinositol 3-kinase/Akt/mammalian target of rapamycin signaling pathway. Infect. Immun. **77:**3919–3931.
7. **Chipuk, J. E., and D. R. Green.** 2008. How do BCL-2 proteins induce mitochondrial outer membrane permeabilization? Trends Cell Biol. **18:**157–164.
8. **De Chiara, G., M. E. Marcocci, M. Torcia, M. Lucibello, P. Rosini, P. Bonini, Y. Higashimoto, G. Damonte, A. Armirotti, S. Amodel, A. T. Palamara, T. Russo, E. Garaci, and F. Cozzolino.** 2006. Bcl-2 phosphorylation by p38 MAPK: identification of target sites and biological consequences. J. Biol. Chem. **281:**21353–21361.
9. **Deng, X., L. Xiao, W. Lang, F. Gao, P. Ruvolo, and W. S. May.** 2001. Novel role for JNK as a stress-activated Bcl2 kinase. J. Biol. Chem. **276:**23681–23688.
10. **Ellgaard, L., and A. Helenius.** 2003. Quality control in the endoplasmic reticulum. Nat. Rev. Mol. Cell Biol. **4:**181–191.
11. **Endo, Y., K. Tsurugi, T. Yutsudo, Y. Takeda, T. Ogasawara, and K. Igarashi.** 1988. Site of action of a Vero toxin (VT2) from *Escherichia coli* O157:H7 and of Shiga toxin on eukaryotic ribosomes: RNA *N*-glycosidase activity of the toxins. Eur. J. Biochem. **171:**45–50.
12. **Falguières, T., and L. Johannes.** 2006. Shiga toxin B-subunit binds to the chaperone BiP and the nucleolar protein B23. Biol. Cell **98:**125–134.
13. **Han, S. W., C. Li, K. O. Ahn, S. W. Lim, H. G. Song, Y. S. Jang, Y. M. Cho, Y. M. Jang, J. Y. Ghee, J. Y. Kim, S. H. Kim, J. Kim, O. J. Kwon, and C. W. Yang.** 2008. Prolonged endoplasmic stress induces apoptotic cell death in an experimental model of chronic cyclosporine nephropathy. Am. J. Nephrol. **28:**707–714.
14. **Harrison, L. M., R. P. Cherla, C. van den Hoogen, W. C. E. van Haaften, S.-Y. Lee, and V. L. Tesh.** 2005. Comparative evaluation of apoptosis induced by Shiga toxin 1 and/or lipopolysaccharides in human monocytic and macrophage-like cells. Microb. Pathog. **38:**63–76.
15. **Haze, K., H. Yoshida, H. Yanagi, T. Yura, and K. Mori.** 1999. Mammalian transcription factor ATF6 is synthesized as a transmembrane protein and activated by proteolysis in response to endoplasmic reticulum stress. Mol. Biol. Cell **10:**3787–3799.
16. **Hengartner, M. O.** 2000. The biochemistry of apoptosis. Nature **407:**770–776.

17. **Iordanov, M. S., D. Pribnow, J. L. Magun, T.-H. Dinh, J. A. Pearson, S. L.-Y. Chen, and B. E. Magun.** 1997. Ribotoxic stress response: activation of the stress-activated protein kinase JNK1 by inhibitors of the peptidyl transferase reaction and by sequence-specific RNA damage to the α-sarcin/ricin loop in the 28S rRNA. Mol. Cell. Biol. **17:**3373–3381.
18. **Ito, T., X. Deng, B. Carr, and W. S. May.** 1997. Bcl2 phosphorylation required for anti-apoptosis function. J. Biol. Chem. **272:**11671–11673.
19. **Karpman, D., A. Håkansson, M. T. R. Perez, C. Isaksson, E. Carlemalm, A. Caprioli, and C. Svanborg.** 1998. Apoptosis of renal cortical cells in the hemolytic-uremic syndrome: in vivo and in vitro studies. Infect. Immun. **66:**636–644.
20. **Kaser, A., A.-H. Lee, A. Franke, J. N. Glickman, S. Zeissig, H. Tilg, E. S. E. Nieuwenhuis, D. E. Higgins, S. Schreiber, L. H. Glimcher, and R. S. Blumberg.** 2008. XBP1 links ER stress to intestinal inflammation and confers genetic risk for human inflammatory bowel disease. Cell **134:**743–756.
21. **Kaufman, R. J.** 2002. Orchestrating the unfolded protein response in health and disease. J. Clin. Investig. **110:**1389–1398.
22. **Lee, A.-H., N. N. Iwakoshi, and L. H. Glimcher.** 2003. XBP-1 regulates a subset of endoplasmic reticulum resident chaperone genes in the unfolded protein response. Mol. Cell. Biol. **23:**7448–7459.
23. **Lee, S.-Y., R. P. Cherla, I. Caliskan, and V. L. Tesh.** 2005. Shiga toxin 1 induces apoptosis in the human myelogenous leukemia cell line THP-1 by a caspase-8-dependent, tumor necrosis factor receptor-independent mechanism. Infect. Immun. **73:**5115–5126.
24. **Lee, S.-Y., R. P. Cherla, and V. L. Tesh.** 2007. Simultaneous induction of apoptotic and survival signaling pathways in macrophage-like THP-1 cells by Shiga toxin 1. Infect. Immun. **75:**1291–1302.
25. **Lee, S.-Y., M.-S. Lee, R. P. Cherla, and V. L. Tesh.** 2008. Shiga toxin 1 induces apoptosis through the ER stress response in human monocytic cells. Cell. Microbiol. **10:**770–780.
26. **Lingwood, C. A.** 2003. Shiga toxin receptor glycolipid binding: pathology and utility. Methods Mol. Med. **73:**165–186.
27. **Luo, R., J.-F. Lu, Q. Hu, and S. N. Maity.** 2008. CBF/NF-Y controls endoplasmic reticulum stress induced transcription through recruitment of both ATF6(N) and TBP. J. Cell. Biochem. **104:**1708–1723.
28. **Martinou, J. C., and D. R. Green.** 2001. Breaking the mitochondrial barrier. Nat. Rev. Mol. Cell Biol. **2:**63–67.
29. **Mathura, V. S., K. V. Soman, T. K. Varma, and W. Braun.** 2003. A multimeric model for murine anti-apoptotic protein Bcl-2 and structural insights for its regulation by post-translational modification. J. Mol. Model. **9:**298–303.
30. **Melton-Celsa, A. R., and A. D. O'Brien.** 1998. Structure, biology, and relative toxicity of Shiga toxin family members for cells and animals, p. 121–128. *In* J. B. Kaper and A. D. O'Brien (ed.), *Escherichia coli* O157:H7 and other Shiga toxin-producing *E. coli* strains. ASM Press, Washington, DC.
31. **Ohmura, M., S. Yamasaki, H. Kurazono, K. Kashiwagi, K. Igarashi, and Y. Takeda.** 1993. Characterization of non-toxic mutants of verotoxin-1 that were constructed by replacing amino acids in the A-subunit. Microb. Pathog. **15:**169–176.
32. **Rao, R. V., H. M. Ellerby, and D. E. Bredesen.** 2004. Coupling endoplasmic reticulum stress to the cell death program. Cell Death Differ. **11:**372–380.
33. **Ruiz-Vela, A., J. T. Opferman, E. H. Cheng, and S. J. Korsmeyer.** 2005. Proapoptotic BAX and BAK control multiple initiator caspases. EMBO Rep. **6:**379–385.
34. **Sandvig, K., S. Grimmer, S. U. Lauvrak, M. L. Torgersen, G. Skretting, B. van Deurs, and T. G. Iversen.** 2002. Pathways followed by ricin and Shiga toxin into cells. Histochem. Cell Biol. **117:**131–141.
35. **Saxena, S. K., A. D. O'Brien, and E. J. Ackerman.** 1989. Shiga toxin, Shiga-like toxin II variant and ricin are all single-site RNA *N*-glycosidases of 28S RNA when microinjected into *Xenopus* oocytes. J. Biol. Chem. **264:**596–601.
36. **Scorrano, L., S. A. Oakes, J. T. Opferman, E. H. Cheng, M. D. Sorcinelli, T. Pozzan, and S. J. Korsmeyer.** 2003. BAX and BAK regulation of endoplasmic reticulum $Ca^{2+}$: a control point for apoptosis. Science **300:**135–139.
37. **Smith, W. E., A. V. Kane, S. T. Campbell, D. W. K. Acheson, B. H. Cochran, and C. M. Thorpe.** 2003. Shiga toxin 1 triggers a ribotoxic stress response leading to p38 and JNK activation and induction of apoptosis in intestinal epithelial cells. Infect. Immun. **71:**1497–1504.
38. **Szegezdi, E., S. E. Logue, A. M. Gorman, and A. Samali.** 2006. Mediators of endoplasmic reticulum stress-induced apoptosis. EMBO Rep. **7:**880–885.
39. **Szegezdi, E., D. C. MacDonald, T. N. Chonghaile, S. Gupta, and A. Samali.** 2009. Bcl-2 family on guard at the ER. Am. J. Physiol. Cell Physiol. **296:**C941–C953.
40. **Tarr, P. I., C. A. Gordon, and W. L. Chandler.** 2005. Shiga toxin producing *Escherichia coli* and the haemolytic uraemic syndrome. Lancet **365:**1073–1086.
41. **Tesh, V. L., J. A. Burris, J. W. Owens, V. M. Gordon, E. A. Wadolkowski, A. D. O'Brien, and J. E. Samuel.** 1993. Comparison of the relative toxicities of Shiga-like toxins type I and type II for mice. Infect. Immun. **61:**3392–3402.
42. **Yoshida, H., T. Okada, K. Haze, H. Yanagi, T. Yura, M. Negishi, and K. Mori.** 2000. ATF6 activated by proteolysis binds in the presence of NF-Y (CBF) directly to the *cis*-acting element responsible for the mammalian unfolded protein response. Mol. Cell. Biol. **20:**6755–6767.
43. **Yu, M., and D. B. Haslam.** 2005. Shiga toxin is transported from the endoplasmic reticulum following interaction with the luminal chaperone HEDJ/ERdj3. Infect. Immun. **73:**2524–2532.

*Editor:* B. A. McCormick